Enhanced second-harmonic generation in AlGaAs/Al_xO_y tightly confining waveguides and resonant cavities

Luigi Scaccabarozzi and M. M. Fejer

Department of Applied Physics, Stanford University, Stanford, California 94305

Yijie Huo and Shanhui Fan

Department of Electrical Engineering, Stanford University, Stanford, California 94305

Xiaojun Yu and James S. Harris

Department of Materials Science, Stanford University, Stanford, California 94305

Received June 26, 2006; revised August 16, 2006; accepted August 16, 2006;
posted September 25, 2006 (Doc. ID 72379); published November 22, 2006

We demonstrate second-harmonic generation (SHG) from sub-micrometer-sized AlGaAs/Al_xO_y artificially birefringent waveguides. The normalized conversion efficiency is the highest ever reported. We further enhanced the SHG using a waveguide-embedded cavity formed by dichroic mirrors. Resonant enhancements as high as ~10× were observed. Such devices could be potentially used as highly efficient, ultracompact frequency converters in integrated photonic circuits. © 2006 Optical Society of America

OCIS codes: 190.4360, 190.2620, 230.5750, 230.7370.

The aluminum gallium arsenide/aluminum oxide (AlGaAs/Al_xO_y) material system is very advantageous for nonlinear optical applications, because of the large nonlinear susceptibility of GaAs (d_{14} = 90 pm/V), the high index contrast, and the mature device fabrication technology. Moreover, active devices can be fabricated on the same substrate leading to the realization of integrated photonic circuits. AlGaAs weakly confining quasi-phase-matched (QPM) waveguides have already been demonstrated[1]; however, they require a complex fabrication process and relatively long interaction length. Recently, artificial birefrigence[2] has been shown to give superior results[3,4] compared to QPM; however, the conversion efficiency remains relatively low due to poor lateral confinement and high loss for the second harmonic (SH).

Here we report SH generation (SHG) in tightly confining, birefringently phase-matched waveguides based on the AlGaAs/Al_xO_y material system. We employed Al_xO_y for achieving both birefringent phase matching and tight confinement. This approach resulted in the highest normalized conversion efficiency reported, to the best of our knowledge, ~20× higher than in previously reported works.[5] We further enhanced the SHG by adding a cavity embedded in the waveguide, resonant at the fundamental wavelength.

The waveguide structure consists of a multilayer core (110 nm $Al_{0.5}Ga_{0.5}As$/90 nm Al_xO_y/110 nm $Al_{0.5}Ga_{0.5}As$) on top of a 2.5 μm thick Al_xO_y cladding. As shown in Fig. 1, the thin Al_xO_y layer does not significantly affect the TE mode profile at the first-harmonic (FH) wavelength but generates large discontinuities in the electric-field distribution of the TM mode (for type II phase matching) at the SH. The SH mode effective index is thus lowered enough to achieve phase matching. The width of the waveguide (typically 800–1000 nm) can be adjusted to shift the phase-matching wavelength to the desired location (typically 1550 nm). The geometrical parameters have been obtained using a finite-difference frequency-domain scheme.[6] The theoretical normalized conversion efficiency for this structure is larger than 20,000%/W/cm^2, more than 100× higher than $LiNbO_3$ nonlinear optical waveguides operating at similar wavelengths.[7]

The layer structure is grown by molecular beam epitaxy (MBE), where $Al_{0.93}Ga_{0.07}As$ is used for the cladding layer. After *e*-beam lithography on thin poly (methyl methacrylate), the pattern is transferred by lift-off to a chromium hard mask. Dry etching in chlorine plasma is used to define the ridge. The sample is then thermally oxidized to convert the $Al_{0.93}Ga_{0.07}As$ to Al_xO_y. The rms sidewall roughness of the fabricated waveguides is less than 6 nm, and the width drift is less than 30 nm over the length of the sample (600 μm), ensuring that the phase-matching condition is maintained.

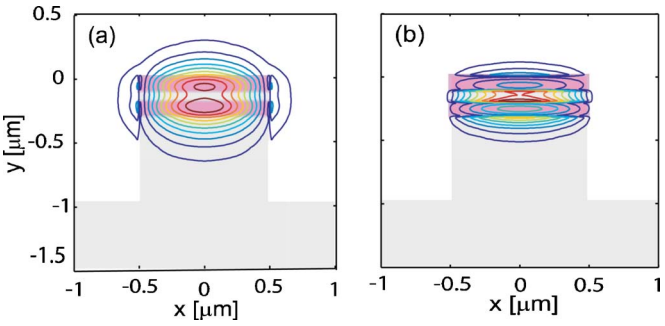

Fig. 1. (Color online) (a) Electric field of fundamental TE and (b) SH TM modes in the waveguide. The effective index of both modes is ~2.2219 at 1.55 μm.

0146-9592/06/243626-3/$15.00

The measurements are conducted using Agilent tunable lasers (81680A and 81640B) in the cw mode, with lock-in detection for the SH. We measure the attenuation coefficient at ~1550 nm using the Fabry–Perot method. The facet reflectivity is 19±1% (for the TE mode) from 3D finite-difference-time-domain simulations, which include the effects of variation of waveguide width and wavelength. The measured loss coefficient is ~2.3±0.7 dB/mm, where the error is due to the uncertainty in the reflectivity calculation and to the experimental fluctuation of the fringe contrast.

From the SH-tuning curve, we determine the phase-matching wavelength for different waveguide widths; the results agree excellently with the simulations, as shown in Fig. 2(a). The single-pass internal conversion efficiency (η') of a waveguide of length L can be experimentally estimated by normalizing the SH output power ($P_{2\omega-o}$) with the squared FH *output* power ($P_{\omega-o}$).[8] This ratio is expressed as

$$\frac{P_{2\omega-\mathrm{out}}}{P^2_{\omega-\mathrm{out}}} = \eta' e^{2\alpha_\omega L}\frac{C_{2\omega-\mathrm{out}}(1-R_{2\omega})}{C^2_{\omega-\mathrm{out}}(1-R_\omega)^2},$$

where α_ω is the FH propagation loss; $(1-R_\omega)$, $(1-R_{2\omega})$ are the FH and SH facet transmissivities; and C_ω and $C_{2\omega}$ are the FH and SH output collection efficiencies. Using the simulated value of $\eta_{\mathrm{norm}}(20{,}000\%/\mathrm{W/cm^2})$, the measured FH loss (2.3 dB/mm), the estimated values (by numerical simulations) of C_ω and $C_{2\omega}$, and assuming no SH loss, we expect to obtain an efficiency η' of 42%/W for a 600 μm long waveguide. Experimentally, we obtain a value of 4%–5%/W, as shown in Fig. 2(b) (0.14 nW of SH collected power with 23 μW of FH output power), comparable to the efficiencies of previously reported birefringent waveguides.[4]

Data fitting results in SH loss of 25–35 dB/mm, where the uncertainty is due to the collection efficiencies of the FH and SH modes. A crude estimation based on the amount of field at the interfaces[9] indicates that the SH loss due to roughness at the horizontal interfaces could be 40–70× larger than the FH loss, for the same amount of roughness. Moreover, the SH mode would be 500–900× more sensitive to roughness at the horizontal interfaces than at the sidewalls. Thus only a small amount of roughness at the horizontal interfaces (due, for example, to the thermal oxidation[10]) could generate high SH loss, indicating an optimal length for the efficiency of 350–400 μm.

The high SH loss is currently the limiting factor to the efficiency of our waveguides. A way to reduce the effect of high loss and to further enhance the conversion efficiency is to build a resonant cavity embedded in the waveguide.

The challenge is to build a mirror that is highly reflective at the fundamental wavelength, while having high transmission at the SH. In fact, typical waveguide distributed Bragg reflectors designed for FH are extremely lossy at the SH, due to the inevitable scattering from the periodic modulation. To solve this problem, we designed a novel mirror structure,

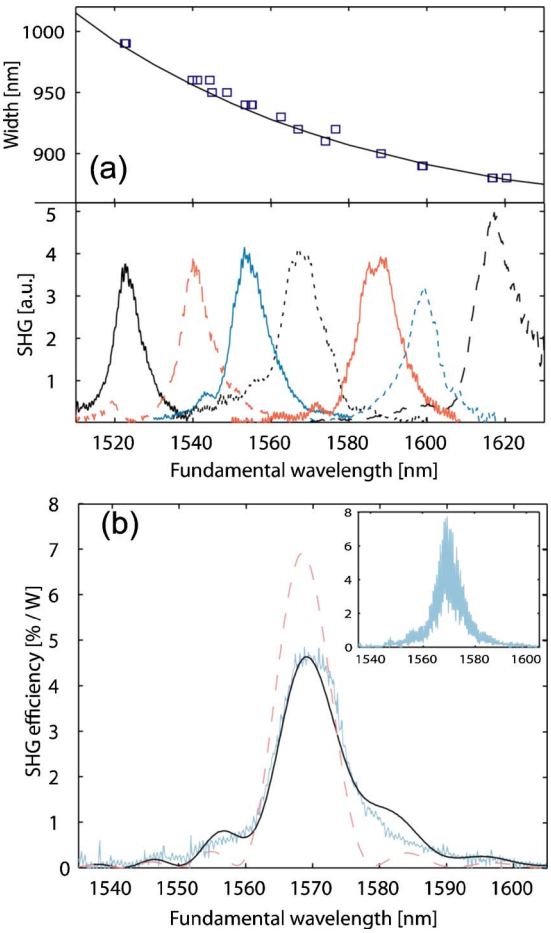

Fig. 2. (Color online) (a) Top, experimental (squares) and simulated (curve) phase-matching wavelength versus waveguide width; bottom, corresponding tuning curves. (b) experimental efficiency [light (blue) solid curve] calculated by normalizing the output SH power to the squared output fundamental power and fitted efficiency with (black solid curve) and without [dashed (purple) curve] taking into account the drift of the effective index. Inset, SH power normalized by the input fundamental power. Note the modulation due to the Fabry–Perot fringes at the fundamental wavelength.

shown in Fig. 3, that exploits the difference in the size of the FH and SH modes by placing the modulation outside of the waveguide. This mirror design can achieve a FH reflectivity as 95% and a SH transmission above 80%. Details of this mirror are published separately.[11]

Using this mirror, we designed a cavity device that is resonant at the (low loss) FH wavelength, which is sufficiently short so that the effect of the SH loss is partially mitigated. Figure 4(a) shows the experimental transmission spectrum of the device at the FH wavelength where the bandgap edges and the cavity modes are visible. The spectrum is complicated by the coupling of the actual cavity (cavity B in Fig. 3) with the two spurious low-finesse cavities formed by the mirrors and the input and output facets (cavities A and C in Fig. 3). To extract the relevant cavity parameters, we fitted the transmission spectrum using a 1D nonlinear transfer-matrix model.[12] This model fits very well with the experimental data [Fig. 4(a) and inset]; in particular, the maximum finesse

matches the experimental estimated finesse of ~7 ($Q \sim 3000$).

Figure 4(b) compares the SH generated in the cavity (80 μm long generating region) with the SH generated by two plain waveguides that are 80 and 400 μm long separately. The particular sample used for this experiment has a slightly different vertical structure, which results in a very broad phase-matching peak that covers the entire spectrum. By comparing the height of these SH spectra, we can estimate a total cavity enhancement of ~5.3 and a total efficiency 50% larger than the highest efficiency achievable with a plain waveguide.

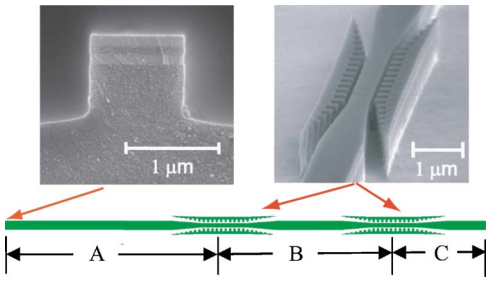

Fig. 3. (Color online) Schematic of the real device structure including the main cavity (B) and the spurious Fabry–Perot cavities (A and C) due to input and output facets. On top are shown scanning electron microscope pictures of the cleaved facet, where the multilayer core is visible, and of the dichroic mirror.

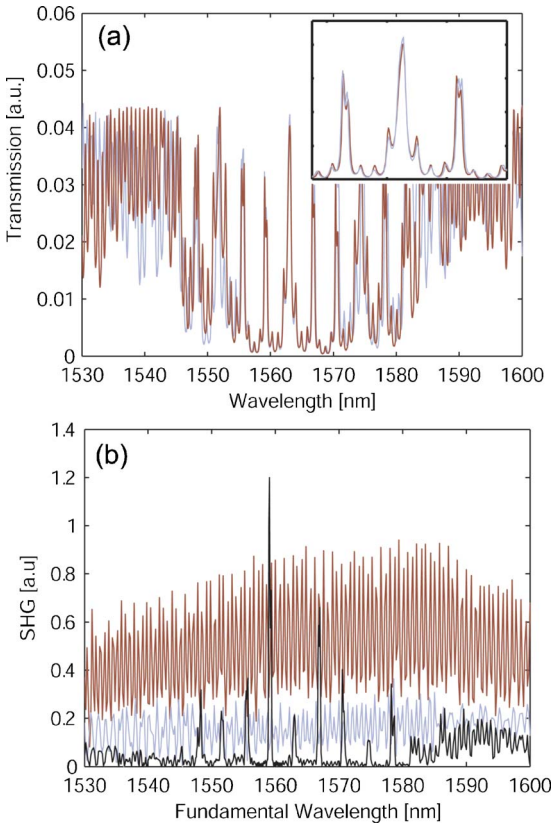

Fig. 4. (Color online) (a) Experimental [blue (light)] and fitted [red (dark)] transmission. Inset, detail of the central portion of the spectrum. (b) SH generated by an 80 μm long cavity (black), and by plain waveguides 80 μm long [blue (light)] and 400 μm long [red (dark)].

These cavities constitute only a proof of concept and not optimal devices. FH spectra of other samples suggest greater than 10× enhancements, which would yield, with the correct layer structure, efficiencies as high as 15%/W. We estimate that, given the actual loss, simply by optimizing the geometrical parameters of the cavity, enhancements greater than ~18× (corresponding to efficiencies as high as 38%/W) should be achievable. Furthermore, we can speculate that, if the FH propagation losses of the waveguide and mirror could be lowered by a factor ~10 (e.g., by improving the quality of the MBE grown crystal or with smoothing-etch techniques), assuming the actual SH loss, enhancements of over 200× should be achievable, comparable with the efficiency of commercial devices (e.g., 1400%/W for 6.45 cm long $LiNbO_3$ waveguides[13]).

In conclusion, we have demonstrated that high normalized conversion efficiency can be obtained with birefringently phase-matched, tightly confining waveguides. The total efficiency is currently limited by the SH loss; however, the use of a short cavity can mitigate the effect of loss and has the potential to produce ultracompact, highly efficient nonlinear optical devices.

We thank Charles and Evans Associates for material analysis. This research was supported by the U.S. Air Force Office of Scientific Research under grant F49620-01-1-0428. Y. Huo's e-mail address is yjhuo@stanford.edu.

References

1. X. Yu, L. Scaccabarozzi, J. S. Harris, P. S. Kuo, and M. M. Fejer, Opt. Express **13**, 10742 (2005).
2. A. Fiore, V. Berger, E. Rosencher, P. Bravetti, and J. Nagle, Nature **391**, 463 (1998).
3. S. V. Rao, K. Moutzouris, and M. Ebrahimzadeh, J. Opt. A **6**, 569 (2004).
4. K. Moutzouris, S. V. Rao, M. Ebrahimzadeh, A. De Rossi, V. Berger, M. Calligaro, and V. Ortiz, Opt. Lett. **26**, 1785 (2001).
5. A. S. Fiore, L. Delobel, P. van der Meer, P. Bravetti, V. Berger, E. Rosencher, and J. Nagle, Appl. Phys. Lett. **72**, 2942 (1998).
6. M. S. Stern, IEE Proc. J **135**, 56 (1988).
7. M. H. Chou, I. Brener, G. Lenz, R. Scotti, E. E. Chaban, J. Shmulovich, D. Philen, S. Kosinski, K. R. Parameswaran, and M. M. Fejer, IEEE Photon. Technol. Lett. **12**, 82 (2000).
8. M. L. Bortz, S. J. Field, M. M. Fejer, D. W. Nam, R. G. Waarts, and D. F. Welch, IEEE J. Quantum Electron. **30**, 2953 (1994).
9. S. G. Johnson, M. I. Povinelli, M. Soljacic, A. Karalis, S. Jacobs, and J. D. Joannopoulos, Appl. Phys. B **81**, 283 (2005).
10. S. Guha, F. Agahi, B. Pezeshki, J. A. Kash, D. W. Kisker, and N. A. Bojarczuk, Appl. Phys. Lett. **68**, 906 (1996).
11. L. Scaccabarozzi, M. M. Fejer, Y. Huo, S. Fan, X. Yu, and J. S. Harris, Opt. Lett. **31**, 3285 (2006).
12. D. S. Bethune, J. Opt. Soc. Am. B **6**, 910 (1989).
13. K. R. Parameswaran, J. R. Kurz, R. V. Roussev, and M. M. Fejer, Opt. Lett. **27**, 43 (2002).